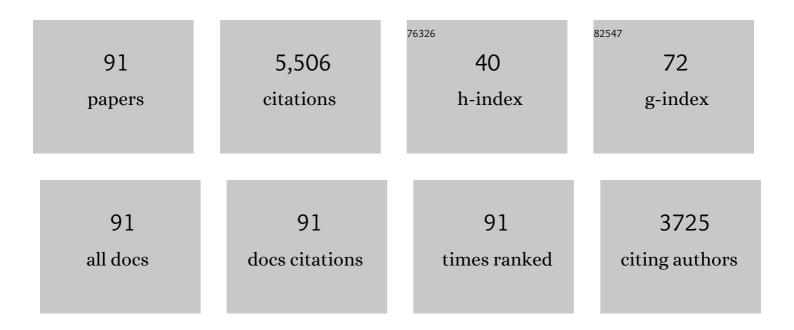
List of Publications by Year in descending order

Source: https://exaly.com/author-pdf/300371/publications.pdf Version: 2024-02-01



Βλιμανίς Υμ

| # | Article | IF | CITATIONS |
|----|--|------|-----------|
| 1 | Automatic building rooftop extraction using a digital surface model derived from aerial stereo images. Journal of Spatial Science, 2022, 67, 21-40. | 1.5 | 13 |
| 2 | Evolution of Urban Spatial Clusters in China: A Graph-Based Method Using Nighttime Light Data. Annals of the American Association of Geographers, 2022, 112, 56-77. | 2.2 | 14 |
| 3 | Snow cover detection in mid-latitude mountainous and polar regions using nighttime light data. Remote Sensing of Environment, 2022, 268, 112766. | 11.0 | 15 |
| 4 | Quantitative Analysis of Urban Polycentric Interaction Using Nighttime Light Data: A Case Study of Shanghai, China. IEEE Journal of Selected Topics in Applied Earth Observations and Remote Sensing, 2022, 15, 1114-1122. | 4.9 | 5 |
| 5 | Evaluation of ICESat-2 ATL03/08 Surface Heights in Urban Environments Using Airborne LiDAR Point Cloud Data. IEEE Geoscience and Remote Sensing Letters, 2022, 19, 1-5. | 3.1 | 4 |
| 6 | The potential of nighttime light remote sensing data to evaluate the development of digital economy: A case study of China at the city level. Computers, Environment and Urban Systems, 2022, 92, 101749. | 7.1 | 51 |
| 7 | The Relationship Between Urban 2-D/3-D Landscape Pattern and Nighttime Light Intensity. IEEE Journal of Selected Topics in Applied Earth Observations and Remote Sensing, 2022, 15, 478-489. | 4.9 | 9 |
| 8 | Evaluating the Ability of NOAA-20 Monthly Composite Data for Socioeconomic Indicators Estimation and Urban Area Extraction. IEEE Journal of Selected Topics in Applied Earth Observations and Remote Sensing, 2022, 15, 1837-1845. | 4.9 | 7 |
| 9 | Assessing the potential and utilization of solar energy at the building-scale in Shanghai. Sustainable Cities and Society, 2022, 82, 103917. | 10.4 | 25 |
| 10 | Evaluation of Vegetation Indexes and Green-Up Date Extraction Methods on the Tibetan Plateau. Remote Sensing, 2022, 14, 3160. | 4.0 | 6 |
| 11 | NPP-VIIRS Nighttime Light Data Have Different Correlated Relationships With Fossil Fuel Combustion Carbon Emissions From Different Sectors. IEEE Geoscience and Remote Sensing Letters, 2021, 18, 2062-2066. | 3.1 | 15 |
| 12 | A spatiotemporal structural graph for characterizing land cover changes. International Journal of Geographical Information Science, 2021, 35, 397-425. | 4.8 | 13 |
| 13 | Improving Satellite Waveform Altimetry Measurements With a Probabilistic Relaxation Algorithm. IEEE Transactions on Geoscience and Remote Sensing, 2021, 59, 4733-4748. | 6.3 | 3 |
| 14 | Spatio-temporal Cokriging method for assimilating and downscaling multi-scale remote sensing data. Remote Sensing of Environment, 2021, 255, 112190. | 11.0 | 10 |
| 15 | An extended time series (2000–2018) of global NPP-VIIRS-like nighttime light data from a cross-sensor calibration. Earth System Science Data, 2021, 13, 889-906. | 9.9 | 286 |
| 16 | A New Method for Building-Level Population Estimation by Integrating LiDAR, Nighttime Light, and POI Data. Journal of Remote Sensing, 2021, 2021, . | 6.7 | 19 |
| 17 | A monthly night-time light composite dataset of NOAA-20 in China: a multi-scale comparison with S-NPP. International Journal of Remote Sensing, 2021, 42, 7931-7951. | 2.9 | 6 |
| 18 | Mapping fine-scale visual quality distribution inside urban streets using mobile LiDAR data. Building and Environment, 2021, 206, 108323. | 6.9 | 17 |

| # | Article | IF | CITATIONS |
|----|---|------|-----------|
| 19 | Analyzing parcel-level relationships between Luojia 1-01 nighttime light intensity and artificial surface features across Shanghai, China: A comparison with NPP-VIIRS data. International Journal of Applied Earth Observation and Geoinformation, 2020, 85, 101989. | 2.8 | 38 |
| 20 | Mapping 3D visibility in an urban street environment from mobile LiDAR point clouds. GIScience and Remote Sensing, 2020, 57, 797-812. | 5.9 | 22 |
| 21 | Urban Building Type Mapping Using Geospatial Data: A Case Study of Beijing, China. Remote Sensing, 2020, 12, 2805. | 4.0 | 23 |
| 22 | Effects of urban forms on CO2 emissions in China from a multi-perspective analysis. Journal of Environmental Management, 2020, 262, 110300. | 7.8 | 62 |
| 23 | Automated Extraction of Street Lights From JL1-3B Nighttime Light Data and Assessment of Their Solar Energy Potential. IEEE Journal of Selected Topics in Applied Earth Observations and Remote Sensing, 2020, 13, 675-684. | 4.9 | 32 |
| 24 | Identifying and evaluating poverty using multisource remote sensing and point of interest (POI) data: A case study of Chongqing, China. Journal of Cleaner Production, 2020, 255, 120245. | 9.3 | 77 |
| 25 | Analysis of Sentinel-3 SAR altimetry waveform retracking algorithms for deriving temporally consistent water levels over ice-covered lakes. Remote Sensing of Environment, 2020, 239, 111643. | 11.0 | 38 |
| 26 | Exploring the relationship between 2D/3D landscape pattern and land surface temperature based on explainable eXtreme Gradient Boosting tree: A case study of Shanghai, China. Science of the Total Environment, 2020, 725, 138229. | 8.0 | 90 |
| 27 | A Spatial-Socioeconomic Urban Development Status Curve from NPP-VIIRS Nighttime Light Data. Remote Sensing, 2019, 11, 2398. | 4.0 | 39 |
| 28 | Siting of Dark Sky Reserves in China Based on Multi-source Spatial Data and Multiple Criteria Evaluation Method. Chinese Geographical Science, 2019, 29, 949-961. | 3.0 | 5 |
| 29 | Applications of Satellite Remote Sensing of Nighttime Light Observations: Advances, Challenges, and Perspectives. Remote Sensing, 2019, 11, 1971. | 4.0 | 171 |
| 30 | Delineating Seasonal Relationships Between Suomi NPP-VIIRS Nighttime Light and Human Activity Across Shanghai, China. IEEE Journal of Selected Topics in Applied Earth Observations and Remote Sensing, 2019, 12, 4275-4283. | 4.9 | 44 |
| 31 | Estimation of Cargo Handling Capacity of Coastal Ports in China Based on Panel Model and DMSP-OLS Nighttime Light Data. Remote Sensing, 2019, 11, 582. | 4.0 | 8 |
| 32 | Mapping Global Urban Areas From 2000 to 2012 Using Time-Series Nighttime Light Data and MODIS Products. IEEE Journal of Selected Topics in Applied Earth Observations and Remote Sensing, 2019, 12, 1143-1153. | 4.9 | 53 |
| 33 | A surface network based method for studying urban hierarchies by night time light remote sensing data. International Journal of Geographical Information Science, 2019, 33, 1377-1398. | 4.8 | 30 |
| 34 | Estimation of Poverty Using Random Forest Regression with Multi-Source Data: A Case Study in Bangladesh. Remote Sensing, 2019, 11, 375. | 4.0 | 95 |
| 35 | Integration of nighttime light remote sensing images and taxi GPS tracking data for population surface enhancement. International Journal of Geographical Information Science, 2019, 33, 687-706. | 4.8 | 62 |
| 36 | Evaluating spatiotemporal patterns of urban electricity consumption within different spatial boundaries: A case study of Chongqing, China. Energy, 2019, 167, 641-653. | 8.8 | 46 |

| # | Article | IF | CITATIONS |
|----|--|------|-----------|
| 37 | Spatiotemporal variations of CO2 emissions and their impact factors in China: A comparative analysis between the provincial and prefectural levels. Applied Energy, 2019, 233-234, 170-181. | 10.1 | 105 |
| 38 | Exploring spatiotemporal patterns of electric power consumption in countries along the Belt and Road. Energy, 2018, 150, 847-859. | 8.8 | 92 |
| 39 | Improving MODIS snow products with a HMRF-based spatio-temporal modeling technique in the Upper Rio Grande Basin. Remote Sensing of Environment, 2018, 204, 568-582. | 11.0 | 49 |
| 40 | An Extended Minimum Spanning Tree method for characterizing local urban patterns. International Journal of Geographical Information Science, 2018, 32, 450-475. | 4.8 | 40 |
| 41 | NPP-VIIRS DNB Daily Data in Natural Disaster Assessment: Evidence from Selected Case Studies. Remote Sensing, 2018, 10, 1526. | 4.0 | 90 |
| 42 | Nighttime Light Images Reveal Spatial-Temporal Dynamics of Global Anthropogenic Resources Accumulation above Ground. Environmental Science & Technology, 2018, 52, 11520-11527. | 10.0 | 22 |
| 43 | Urban Built-Up Area Extraction From Log- Transformed NPP-VIIRS Nighttime Light Composite Data. IEEE Geoscience and Remote Sensing Letters, 2018, 15, 1279-1283. | 3.1 | 102 |
| 44 | Estimation of snow accumulation over frozen Arctic lakes using repeat ICESat laser altimetry observations – A case study in northern Alaska. Remote Sensing of Environment, 2018, 216, 529-543. | 11.0 | 10 |
| 45 | Mapping annual urban dynamics (1985–2015) using time series of Landsat data. Remote Sensing of Environment, 2018, 216, 674-683. | 11.0 | 101 |
| 46 | A New Approach for Detecting Urban Centers and Their Spatial Structure With Nighttime Light Remote Sensing. IEEE Transactions on Geoscience and Remote Sensing, 2017, 55, 6305-6319. | 6.3 | 144 |
| 47 | Analysis of Thermal Structure of Arctic Lakes at Local and Regional Scales Using in Situ and Multidate Landsatâ€8 Data. Water Resources Research, 2017, 53, 9642-9658. | 4.2 | 24 |
| 48 | A Graph-Based Approach for 3D Building Model Reconstruction from Airborne LiDAR Point Clouds. Remote Sensing, 2017, 9, 92. | 4.0 | 58 |
| 49 | Urban Expansion and Agricultural Land Loss in China: A Multiscale Perspective. Sustainability, 2016, 8, 790. | 3.2 | 83 |
| 50 | View-based greenery: A three-dimensional assessment of city buildings' green visibility using Floor Green View Index. Landscape and Urban Planning, 2016, 152, 13-26. | 7.5 | 96 |
| 51 | A graph-based approach for assessing storm-induced coastal changes. International Journal of Remote Sensing, 2016, 37, 4854-4873. | 2.9 | 4 |
| 52 | Individual tree crown delineation using localized contour tree method and airborne LiDAR data in coniferous forests. International Journal of Applied Earth Observation and Geoinformation, 2016, 52, 82-94. | 2.8 | 60 |
| 53 | Intra-urban differences of mean radiant temperature in different urban settings in Shanghai and implications for heat stress under heat waves: A GIS-based approach. Energy and Buildings, 2016, 130, 829-842. | 6.7 | 68 |
| 54 | Detecting spatiotemporal dynamics of global electric power consumption using DMSP-OLS nighttime stable light data. Applied Energy, 2016, 184, 450-463. | 10.1 | 159 |

| # | Article | IF | CITATIONS |
|----|---|------|-----------|
| 55 | Revealing the early ice flow patterns with historical Declassified Intelligence Satellite Photographs back to 1960s. Geophysical Research Letters, 2016, 43, 5758-5767. | 4.0 | 18 |
| 56 | Modeling spatiotemporal CO2 (carbon dioxide) emission dynamics in China from DMSP-OLS nighttime stable light data using panel data analysis. Applied Energy, 2016, 168, 523-533. | 10.1 | 222 |
| 57 | Automated extraction of ground surface along urban roads from mobile laser scanning point clouds. Remote Sensing Letters, 2016, 7, 170-179. | 1.4 | 48 |
| 58 | Estimating Roof Solar Energy Potential in the Downtown Area Using a GPU-Accelerated Solar Radiation Model and Airborne LiDAR Data. Remote Sensing, 2015, 7, 17212-17233. | 4.0 | 48 |
| 59 | Poverty Evaluation Using NPP-VIIRS Nighttime Light Composite Data at the County Level in China. IEEE Journal of Selected Topics in Applied Earth Observations and Remote Sensing, 2015, 8, 1217-1229. | 4.9 | 204 |
| 60 | Analysis of water temperature variability of Arctic lakes using Landsat-8 data. , 2015, , . | | 0 |
| 61 | A multistage collaborative 3D GIS to support public participation. International Journal of Digital Earth, 2015, 8, 212-234. | 3.9 | 25 |
| 62 | Modeling and mapping total freight traffic in China using NPP-VIIRS nighttime light composite data. GIScience and Remote Sensing, 2015, 52, 274-289. | 5.9 | 94 |
| 63 | A localized contour tree method for deriving geometric and topological properties of complex surface depressions based on high-resolution topographical data. International Journal of Geographical Information Science, 2015, 29, 2041-2060. | 4.8 | 52 |
| 64 | Extracting and understanding urban areas of interest using geotagged photos. Computers, Environment and Urban Systems, 2015, 54, 240-254. | 7.1 | 232 |
| 65 | Mapping Vegetation-Covered Urban Surfaces Using Seeded Region Growing in Visible-NIR Air Photos. IEEE Journal of Selected Topics in Applied Earth Observations and Remote Sensing, 2015, 8, 2212-2221. | 4.9 | 7 |
| 66 | Estimating House Vacancy Rate in Metropolitan Areas Using NPP-VIIRS Nighttime Light Composite Data. IEEE Journal of Selected Topics in Applied Earth Observations and Remote Sensing, 2015, 8, 2188-2197. | 4.9 | 112 |
| 67 | Evaluating the Ability of NPP-VIIRS Nighttime Light Data to Estimate the Gross Domestic Product and the Electric Power Consumption of China at Multiple Scales: A Comparison with DMSP-OLS Data. Remote Sensing, 2014, 6, 1705-1724. | 4.0 | 481 |
| 68 | Investigating the Temporal and Spatial Variability of Total Ozone Column in the Yangtze River Delta Using Satellite Data: 1978–2013. Remote Sensing, 2014, 6, 12527-12543. | 4.0 | 13 |
| 69 | Multi-Level Spatial Analysis for Change Detection of Urban Vegetation at Individual Tree Scale. Remote Sensing, 2014, 6, 9086-9103. | 4.0 | 29 |
| 70 | Evaluation of NPP-VIIRS night-time light composite data for extracting built-up urban areas. Remote Sensing Letters, 2014, 5, 358-366. | 1.4 | 289 |
| 71 | Object-based spatial cluster analysis of urban landscape pattern using nighttime light satellite images: a case study of China. International Journal of Geographical Information Science, 2014, 28, 2328-2355. | 4.8 | 180 |
| 72 | Normalization of time series DMSP-OLS nighttime light images for urban growth analysis with Pseudo Invariant Features. Landscape and Urban Planning, 2014, 128, 1-13. | 7.5 | 109 |

| # | Article | IF | CITATIONS |
|----|---|-----|-----------|
| 73 | A geospatial web portal for sharing and analyzing greenhouse gas data derived from satellite remote sensing images. Frontiers of Earth Science, 2013, 7, 295-309. | 2.1 | 3 |
| 74 | Validation of total ozone column derived from OMPS using ground-based spectroradiometer measurements. Remote Sensing Letters, 2013, 4, 937-945. | 1.4 | 4 |
| 75 | Toward automatic estimation of urban green volume using airborne LiDAR data and high resolution Remote Sensing images. Frontiers of Earth Science, 2013, 7, 43-54. | 2.1 | 76 |
| 76 | A Voxel-Based Method for Automated Identification and Morphological Parameters Estimation of Individual Street Trees from Mobile Laser Scanning Data. Remote Sensing, 2013, 5, 584-611. | 4.0 | 189 |
| 77 | Locating suitable roofs for utilization of solar energy in downtown area using airborne LiDAR data and object-based method: A case study of the Lujiazui region, Shanghai. , 2012, , . | | 6 |
| 78 | Voxel-based Marked Neighborhood Searching method for identifying street trees using Vehicle-borne Laser Scanning data. , 2012, , . | | 4 |
| 79 | Analyzing spatio-temporal distribution of crime hot-spots and their related factors in Shanghai, China. , 2011, , . | | 6 |
| 80 | Application of ArcGIS in fractal analysis of rivers. , 2011, , . | | 1 |
| 81 | An integrated framework for retrieving and analyzing geographic information in web pages. , 2011, , . | | Ο |
| 82 | A solution for the data collection in the field survey based on Mobile and Wireless GIS. , 2010, , . | | 6 |
| 83 | A method for representing thematic data in three-dimensional GIS. , 2010, , . | | 2 |
| 84 | Mobile and Wireless GIS Based Upon Independent Development. , 2010, , . | | 2 |
| 85 | Spatial indexing of global geographical data with HTM. , 2010, , . | | 2 |
| 86 | Automated derivation of urban building density information using airborne LiDAR data and object-based method. Landscape and Urban Planning, 2010, 98, 210-219. | 7.5 | 200 |
| 87 | An Approach for Integrating Geospatial Processing Services into Three-Dimensional GIS. Lecture Notes in Computer Science, 2010, , 154-161. | 1.3 | 2 |
| 88 | Investigating impacts of urban morphology on spatio-temporal variations of solar radiation with airborne LIDAR data and a solar flux model: a case study of downtown Houston. International Journal of Remote Sensing, 2009, 30, 4359-4385. | 2.9 | 65 |
| 89 | An object-based two-stage method for a detailed classification of urban landscape components by integrating airborne LiDAR and color infrared image data: A case study of downtown Houston. , 2009, , . | | 11 |
| 90 | Object-based algorithms and methods for quantifying urban growth pattern using sequential satellite images. , 2008, , . | | 1 |

| # | Article | IF | CITATIONS |
|----|---|-----|-----------|
| 91 | Simulating and Mapping the Variations of Solar Radiation at the Lujiazui Region of Shanghai Using Airborne LiDAR Data. Key Engineering Materials, 0, 500, 511-516. | 0.4 | 3 |